

Preliminary analysis of immunoregulatory mechanism of hyperhomocysteinemia-induced brain injury in Wistar-Kyoto rats

YU ZHANG¹, LIN WANG¹, XIN LI¹ and JIE GENG²

¹Department of Geriatrics, The Second Hospital of Tianjin Medical University;

²Department of Cardiology, Tianjin Chest Hospital, Tianjin 300211, P.R. China

Received August 2, 2020; Accepted February 5, 2021

DOI: 10.3892/etm.2021.9914

Abstract. Hyperhomocysteinemia (HHcy) can be used as an independent risk factor for predicting cardiovascular disease, stroke and vitamin B12 deficiency. Patients with HHcy have elevated plasma homocysteine (Hcy) concentrations. Enhancing cerebrovascular permeability of substances such as Hcy and brain damage will synergistically increase the symptoms of hypertension, but the specific immune regulation mechanism is still not clear. The purpose of the present study was to preliminarily explore the immunomodulatory mechanism of brain damage caused by HHcy in Wistar-Kyoto (WKY) rats. A total of 60 WKYs were randomly divided into three groups: WKY control group (WKY-C group), WKY methionine group (WKY-M group) and WKY treatment group (WKY-T group; vitamin B6, B12 and folic acid were used as treatment), with 20 rats in each group. Physical examination of body weight, systolic blood pressure (SBP) and plasma Hcy content was performed routinely. The concentration of cytokines, including IL-6, IL-10, IL-17A and TGF- β , associated with T helper cell 17 (Th17) and regulatory T (Treg) cells and key regulator genes, including retinoic acid-related orphan receptor γ t (ROR γ t) and forkhead box P3 (FoxP3), were detected by ELISA, reverse transcription-quantitative PCR and western blotting. Th17/Treg lymphocytes were determined by flow cytometry. MRI scan was preliminarily used to detect the changes characteristic of the ischemic stroke. The results revealed that high methionine diets might have a significant effect on the body weight and SBP. The inflammatory response effect of Treg cells was significantly inhibited in the WKY-M group, and that of Th17 cells was

upregulated when compared to the WKY-T group. Compared with the WKY-T group, the expression levels of IL-17A and ROR γ t in the WKY-M group were significantly upregulated, while the mRNA levels of FoxP3 in the WKY-M group were significantly downregulated. The diet intervention (including vitamins B6 and B12 and folic acid) could reduce the level of Hcy in the blood, but also reduce the inflammatory response and rectify the Treg/Th17 immune imbalance to ameliorate the brain tissue damage. In conclusion, the present study indicated that HHcy can promote inflammation by triggering Treg/Th17 immune imbalance to ameliorate the brain tissue damage.

Introduction

Homocysteine (Hcy) is a thiol-containing amino acid, and an intermediate product of methionine and cysteine amino acid metabolism (1-3). Hcy was first isolated from bladder stones in 1931 and was thought to be related to the development of atherosclerosis as early as in 1969 (4). When the metabolic pathway is altered due to genetic or acquired factors, the Hcy level increases, exceeding maximum normal levels, leading to a condition termed hyperhomocysteinemia (HHcy) (5,6). HHcy is used as an independent risk factor for predicting cardiovascular disease, stroke and vitamin B12 deficiency (7-9). Research to date has indicated that the two most important systems affected by HHcy are the cardiovascular and nervous systems.

Studies have found that Hcy plays an important role in the occurrence and development of carotid atherosclerosis (10-12). Elevated plasma levels of Hcy are associated with asymptomatic carotid artery disease in patients with hypertension. Stroke, head trauma and pressure cause the blood-brain barrier (BBB) to be destroyed, exposing the brain to plasma components, including Hcy (13-17). Hcy also mediates cardiovascular conditions due to its adverse effects on the cardiovascular endothelium and smooth muscle cells, leading to changes in subclinical arterial structure and function (13-15). In addition, acute ischemic stroke seems to be associated with the increase in inflammatory cytokine levels induced by Hcy and the permeability of the BBB (16-17). Through this mechanism, studies have found that multivitamin therapy can protect the BBB against damage by reducing plasma Hcy levels (18-20). In addition, the activation of the inflammatory cascade following brain lesions can trigger changes in the human immune system,

Correspondence to: Dr Jie Geng, Department of Cardiology, Tianjin Chest Hospital, 93 Xi'an Road, Heping, Tianjin 300211, P.R. China
E-mail: gengjie_1973@126.com

Dr Xin Li, Department of Geriatrics, The Second Hospital of Tianjin Medical University, 23 Pingjiang Road, Hexi, Tianjin 300211, P.R. China
E-mail: jessielx@126.com

Key words: homocysteine, hyperhomocysteinemia, brain injury, immune imbalance

and different inflammatory cells play differential roles (21,22). T helper cell 17 (Th17) and regulatory T cells (Tregs) play an important role in maintaining the immune balance (23). Th17 cells secrete high levels of IL-17A, which mainly mediates the inflammatory response and can promote the maturation, proliferation and chemotaxis of neutrophils (23-25). Tregs secrete certain inhibitory cytokines, such as IL-10, IL-4 and TGF- β , which mainly mediate immune tolerance and play an important role in maintaining the body's immune balance (24,25). Th17 and Tregs antagonize each other in function and differentiation (24). When the body is in a normal state, the two maintain a relative balance; however, but when the body is in an abnormal state, an imbalance occurs between Th17 and Tregs. On the other hand, CD4⁺ T cells can differentiate into various Tregs, which can suppress adaptive T cell responses and prevent autoimmunity (25). The control of the Th17/Treg balance is also crucial to the development of inflammatory diseases and the inflammatory response in brain lesions (24,25). In addition, it has been indicated that transcription factors, such as retinoic acid-related orphan receptor γ t (ROR γ t) and forkhead box P3 (FoxP3) play an important role in Th17 and Tregs cells (26,27). This suggests that Th17 and Tregs should not only be analyzed, but also the underlying mechanism and the regulatory network involved should be considered. Th17 and Tregs have been extensively investigated in the context of the inflammatory response following brain injury; however, the role of the two in the brain ischemic inflammatory response remains controversial (28,29). This is not only due to the interdependence between the nervous system and the immune system, but also due to the different response of the two systems in the process of brain ischemic inflammation.

In the present study, an animal model of HHcy was established using Wistar-Kyoto (WKY) rats administered a high methionine diet. The rats were then fed with a therapeutic diet (including vitamins B6 and B12, and folic acid). Changes in body weight, systolic blood pressure and plasma Hcy contents were observed in the rats. In addition, the levels of inflammatory cytokines (IL-6, IL-17A, IL-10 and TGF- β) associated with Th17 and Tregs were detected, and changes in the plasma levels of Th17 and Tregs, as well as key transcription factor (ROR γ t and FoxP3) expression in brain tissue were determined to assess brain tissue damage and the systemic immune response.

Materials and methods

Construction of animal models and animal welfare. A total of 60 male WKYs (weight, 185.3-228.6 g; age, 8 weeks) were purchased from the Laboratory Animal Center of the Chinese Academy of Military Medical Sciences. All animal experiments were approved by the Animal Experiment Ethics Committee of the Second Hospital of Tianjin Medical University (Tianjin, China). All animals were allowed food and water *ad libitum* and were housed under conditions of a 12-h light/dark cycle (lights on at 7:00 a.m.) at a temperature of 22°C with 40-60% humidity. The experiments were carried out in accordance with the National Institutes of Health Guide for the Care and use of Laboratory Animals (30). For inhalant anesthesia during the physical examination procedures,

after 3% anesthetic induction, anesthesia maintenance with 1.5% isoflurane (Macklin Inc.) was used for each rat. At the end of the experiment, all rats were euthanized by intraperitoneal injection of sodium pentobarbital (80 mg/kg; cat. no. P-010; Cerilliant Corporation), and exsanguination was used to euthanize them, and blood samples were collected according to the AVMA Guidelines on the Euthanasia of Animals (31). Brain tissues were removed and immediately frozen in liquid nitrogen and stored at -80°C.

A total of 60 WKYs were randomly divided into three groups: WKY control group (WKY-C group), WKY methionine group (WKY-M group) and WKY treatment group (WKY-T group), with 20 rats in each group. The experiment was intended to intervene in animal feeding conditions for 16 weeks. Throughout the experiment, WKY-C rats were given normal animal feed (without methionine), while WKY-M and WKY-T rats received 2% methionine-supplemented (cat. no. M9500; Merck KGaA) feed. Starting from the first day of week 9, WKY-T rats were treated by gavage daily for 8 weeks, with a regimen of 12 mg/kg vitamin B6 (cat. no. P5669), 0.09 mg/kg vitamin B12 (cat. no. V2876), and 4 mg/kg folic acid (cat. no. F7876; all from Merck KGaA). At the same time, the WKY-M and WKY-C groups received normal saline for 8 weeks. The dose was adjusted and calculated according to the weight change of each rat.

Physical examination and plasma Hcy analysis. The body weights of rats were measured and recorded on the first day (week 0) and weeks 4, 8, 12 and 16. At the same time, a non-invasive blood pressure measurement system was used to monitor the systolic blood pressure (SBP) of the tail artery in the state of consciousness (Taimen BP-100A automatic large-scale non-invasive blood pressure measurement system; Chengdu Taimeng Software Co., Ltd.). In order to ensure the accuracy of the SBP measurement, the temperature of each rat was controlled at 37°C, the blood pressure of each rat was measured three times after obtaining a stable baseline (Taimen BP-100A small animal heater; Chengdu Taimeng Software Co., Ltd.). The plasma Hcy concentrations in WKYs were determined by a 7500B automatic immunobiochemical analyzer (Applied Biosystems; Thermo Fisher Scientific, Inc.) following the manufacturer's instructions.

Cytokine release assay. Starting at the 9th week of gastric gavage treatment for the WKY-T group, the tail blood of the rats in all groups was collected by centrifugation every 4 weeks. The collected blood samples were centrifuged at 4°C at 1,500 x g for 10 min to collect serum. The cytokine concentrations of IL-17A (cat. no. DY8410-05), IL-6 (cat. no. DY506), IL-10 (cat. no. DY522) and TGF- β (cat. no. PMB100B; all from R&D Systems, Inc.) in peripheral blood were measured by ELISA. Each sample was tested in triplicate. The OD value of each well was measured at a wavelength of 450 nm within 15 min. The concentration was calculated according to the manufacturer's instructions.

Flow cytometric analysis. Th17/Treg lymphocytes were determined by flow cytometry. The peripheral blood samples of WKY-C/M/T rats were selected for analysis at weeks 0, 4, 8, 12 and 16. Briefly, peripheral venous blood (1 ml) was

Table I. The mRNA primers of this study.

Target gene	Primer direction	Primer sequence (5'-3')
IL-17A	Forward	GCAGCGGTACTCATCCCTCAA
	Reverse	TCATTGCGGCTCAGAGTCCAG
ROR γ t	Forward	GAACCAGAACAGGGCTCAGAC
	Reverse	TAGAAGGTCTCCAGGCGTAG
IL-10	Forward	ACGCTGTTCATCGATTCTCCC
	Reverse	TCCCACACTCCAGGTTCCGGTC
FoxP3	Forward	CCCTTTCACCTATGCCACCCT
	Reverse	TTGTGGCGGATGGCATTCTTC
β -actin	Forward	TCAGGTCATCACTATCGGCAA
	Reverse	AGCACTGTGTTGGCATAGAGG

ROR γ t, retinoic acid-related orphan receptor γ t; FoxP3, forkhead box P3.

collected in anticoagulation tubes and mixed with 1 ml of PBS (cat. no. P1020; Beijing Solarbio Science & Technology Co., Ltd.). The PBS liquid was then slowly added to the wall of the tube and centrifuged at 4°C, 500 x g for 20 min. Following centrifugation, the lymphocyte layer was collected into a new tube. Subsequently, 1ml PBS solution was added, and the mixture was centrifuged at 4°C, 500 x g for 10 min. After discarding the supernatant, the cells were washed twice with PBS, and prepared to perform flow cytometric analysis. CD3-APC (cat. no. 17-0030-82; clone, eBioG4.18), CD4-PC5 (cat. no. 15-0041-82; clone, GK1.5), CD25-FITC (cat. no. MA1-35144; clone, CD25-3G10), FoxP3-PE (cat. no. 12-5773-82; clone, FJK-16s) and IL-17A-PC7 (cat. no. 25-7177-82; clone, eBio17B7) antibodies were purchased from eBioscience; Thermo Fisher Scientific, Inc. The isotype controls were used as follows: Rat IgG2b κ isotype control PE-Cyanine5 (clone, eB149/10H5; cat. no. 15-4031-82; eBioscience); Mouse IgG2b κ isotype control FITC (clone, eBMG2b; cat. no. 11-4732-81; eBioscience); Rat IgG2a κ isotype control PE (clone, eBR2a; cat. no. 12-4321-80; eBioscience); Rat IgG2a κ isotype control PE-Cyanine7 PE (clone, eBR2a; cat. no. 25-4321-82; eBioscience). The cells were incubated with indicated antibodies at 4°C for 20 min and then washed once with PBS and resuspended in PBS. For intracellular staining of FoxP3, 1.0 ml 1X fixation/permeabilization solution (Foxp3 Transcription Factor Fixation/Permeabilization Concentrate and Diluent; cat. no. 00-5521-00; eBioscience) was added to each tube, which was vortexed and incubated at 4°C for 60 min in the dark. Following incubation, 1X permeabilization buffer solution (10X Permeabilization Buffer; eBioscience, Inc.) was added to each tube, and the tubes were vortexed and washed two times and centrifuged at 4°C, 400 x g for 10 min. The supernatant was subsequently removed, and 5.0 μ l FoxP3-PE antibody (cat. no. 11-5773; eBioscience, Inc.) was added. Cells were run on a CyAn ADP flow cytometer (Beckman Coulter, Inc.) for flow cytometry. Treg cells were characterized as the percentage of CD25⁺FoxP3⁺, and Th17 cells as the percentage of CD4⁺IL17⁺ cells among the CD3⁺CD4⁺ cell population. Data were analyzed using Flow Jo software (version 10.4; FlowJo LLC). Positive and negative cell populations for each marker were determined using fluorescence controls and

unstained cells were used as a negative control. Instrument settings were verified and adjusted with the mid-peak bead of the eight-peak calibration bead set (Spherotech Inc.) before each acquisition session. Compensation beads (BD Biosciences) were used to correct for spectral overlap between channels, as previously described (32).

Reverse transcription-quantitative PCR (RT-qPCR). Total RNA was isolated from ~40 mg brain tissues using TRIzol[®] reagent (Invitrogen; Thermo Fisher Scientific, Inc.) according to the manufacturer's instructions. Total RNA (~5 μ g) of with oligo (dT) primers was reverse transcribed in a 20- μ l volume using the RevertAid First Strand cDNA Synthesis kit (Thermo Fisher Scientific, Inc.) according to the manufacturer's instructions. qPCR was performed using an ABI PRISM 7000 Sequence Detection System (Applied Biosystem; Thermo Fisher Scientific, Inc.). The reactions were set up as follows: 10 μ l FastStart Universal SYBR Green Master (cat. no. 4913850001; Roche Diagnostics), 0.4 μ l forward primer, 0.4 μ l reverse primer, 1 μ l cDNA template and 8.2 μ l ddH₂O, for a total reaction volume of 20 μ l. The reaction system was preheated at 95°C for 10 min, followed by 40 cycles of 95°C for 15 sec and 72°C for 30 sec. After gene amplification, the melting and amplification curves of the target genes were recorded. Expression levels of target genes were calculated using the 2^{- Δ ACq} method with β -actin control (33). All experiments were repeated three times. The IL-17A, ROR γ t, IL-10, FoxP3 and β -actin-specific primers are listed in Table I. The PCR primers were selected from different exons of the corresponding genes to discriminate PCR products that might arise from possible chromosomal DNA contaminants.

Western blot analysis. At week 16, the total protein was extracted from brain tissues, and the protein expression of ROR γ t and FoxP3 was detected by western blotting. RIPA protein lysis buffer (cat. no. R0020; Beijing Solarbio Science & Technology Co., Ltd.) and protease inhibitor were used to extract tissue protein. The volume ratio of RIPA and protease inhibitor was 100:1. Bradford assay (Pierce Bradford Assay kit; Pierce; Thermo Fisher Scientific, Inc.) was used to measure the

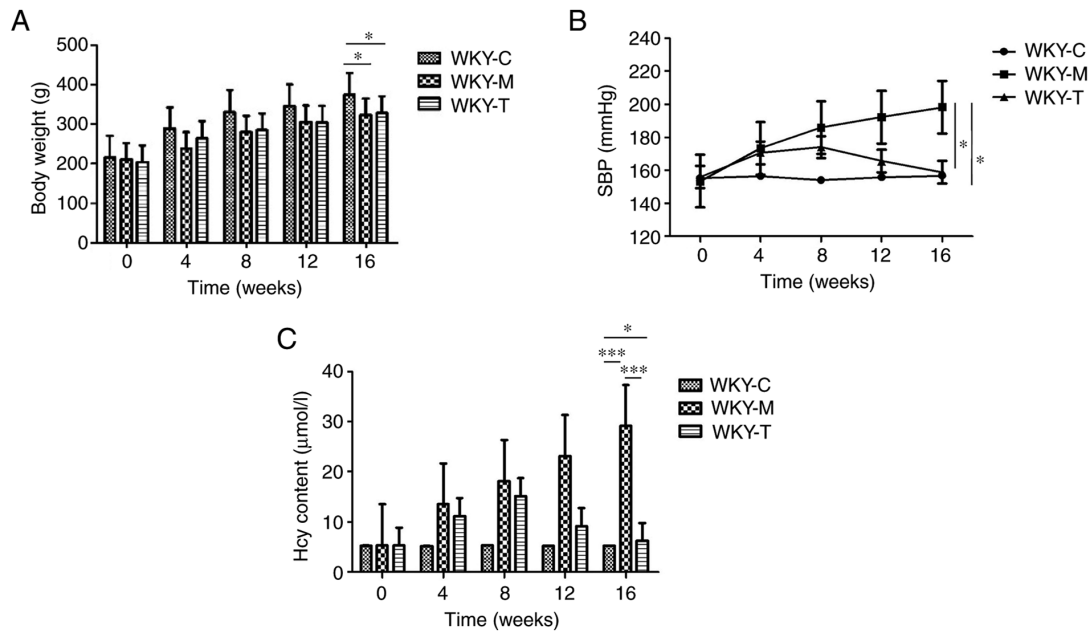


Figure 1. Physical examination and detection of plasma Hcy content. (A) Body weight, (B) SBP and (C) plasma Hcy content changes over the 16 weeks in each group. Data are presented as the mean \pm standard error of the mean. * P <0.05 and *** P <0.001 as indicated. SBP, systolic blood pressure; Hcy, homocysteine; C, control; M, methionine; T, treatment; WKY, Wistar-Kyoto.

protein concentration at 595 nm. Equal amount (10 μ g/lane) proteins from each group were separated by 10% SDS-PAGE and then transferred onto a polyvinylidene fluoride membrane. The membrane was blocked with 5% fat-free milk for 1 h at room temperature. Membranes were then incubated with specific primary antibodies against FoxP3 (cat. no. ab215206; 1:800 dilution; Abcam), ROR γ t (cat. no. ab207082; 1:1,000 dilution; Abcam) and actin (cat. no. ab179467; 1:5,000 dilution; Abcam) overnight at 4°C. Then membranes were incubated with a secondary antibody (goat anti-rabbit IgG HRP-linked; cat. no. ab6721; 1:10,000 dilution; Abcam) for 1 h at room temperature. Enhanced chemiluminescence reagent (cat. no. 32106; Thermo Fisher Scientific, Inc.) was used to visualize bands with a Tanon WB camera (Tanon Science and Technology Co., Ltd.). ImageJ software (version, 1.53d_19; National Institutes of Health) was used to perform densitometry analysis to quantify the protein expression (34). All experiments were repeated three times.

MRI. A 7.0T MRI small animal magnetic resonance scanner (Bruker Corporation) was used for MRI analysis. The selected scan sequences included fast spin echo T1WI sequence and T2WI sequence, both with the coronal scan, as commonly used in rats (35). A total of 12 rats in the WKY-C, WKY-M and WKY-T groups at 24 weeks of age were selected, and 3 rats in each group were subjected to routine head MRI examination. Continuous respiratory anesthesia was performed using 2% isoflurane mixed with 98% oxygen, followed by MRI scan under anesthesia. The following parameters were used: Scan range, full head; tuning, <200 MHz prior to scanning; shimming, 100 MHz. The scan parameters were as follows: T2WI sequence imaging parameters: Repetition time (TR), 3000 msec; echo time (TE), 75 msec; echo train length (ETL), 8; layer thickness, 1.5 mm; layer spacing, 0.2 mm; number of the excitation (NEX), 4; matrix, 256x256; field of

view (FOV), 35x35 mm; imaging time, ~6 min and 30 sec. T1WI sequence imaging parameters were as follows: TR, 500 msec; TE, 17 msec; layer thickness, 1.5 mm, layer spacing, 0.2 mm; NEX, 3; matrix, 256x256; FOV, 35x35 mm; imaging time, ~5 min and 15 sec.

Statistical analysis. All animals were randomized into three groups. The results are presented as the mean \pm standard error of the mean. The experiments (including physical examination, ELISA, RT-qPCR and flow cytometric analysis) were repeated three times. Statistical analysis was performed using GraphPad Prism 6.0 software (GraphPad Software, Inc.). Differences between three groups were measured using one-way ANOVA with Tukey's post hoc test. P <0.05 was considered to indicate a statistically significant difference.

Results

Detection of body weight and plasma Hcy content. In order to explore the preliminary effects of a high methionine diet, a statistical analysis of the body weights of WKY rats was conducted (Fig. 1A). The overall observation was that the weights of the rats in the three groups during the 16-week period exhibited a gradual upward trend. The results revealed that from 0 to 16 weeks, the rats in the WKY-C group exhibited the heaviest weight and the most rapid increase in weight. The amplitudes of body weight of the rats in the WKY-M group ($n=20$) and WKY-T ($n=20$) group were lower than those in the WKY-C ($n=20$) group. The WKY-M group exhibited the highest SBP level, which was higher than the baseline of the WKY-C group (Fig. 1B). Following treatment, it was observed that the SBP value began to gradually decrease in the WKY-T group and was significantly lower than that in the WKY-M group at week 16. To further investigate the effects of a high methionine diet and to confirm the successful

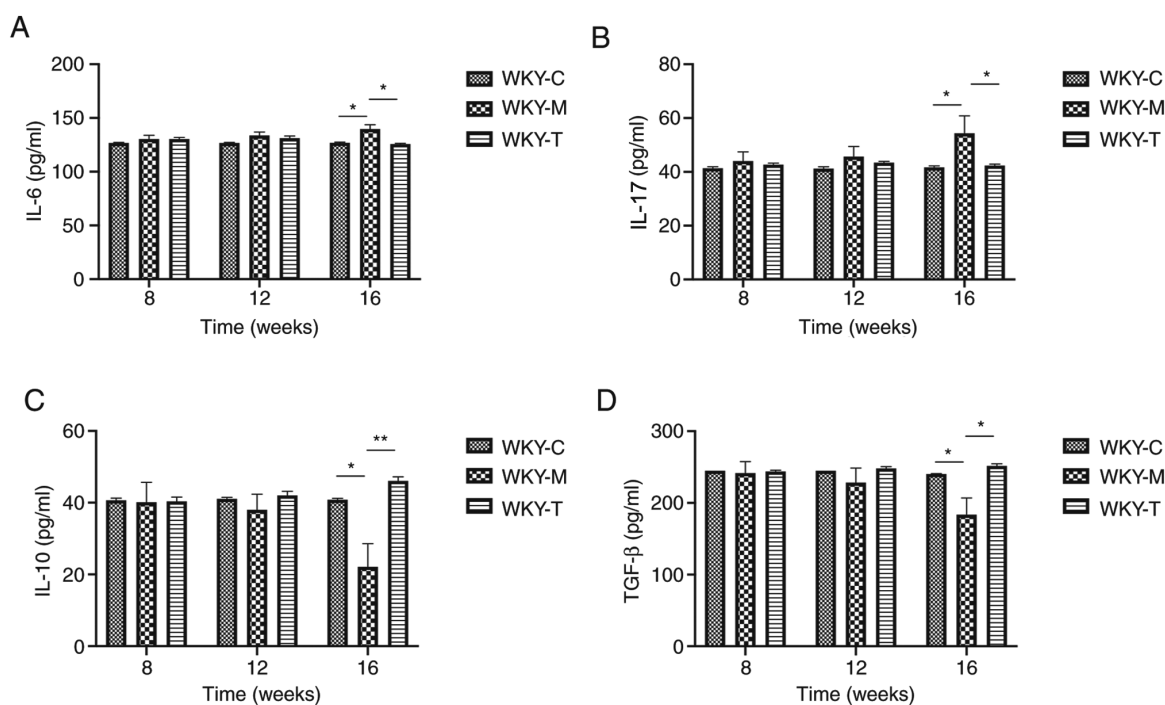


Figure 2. Cytokine release analysis. The plasma expression of (A) IL-6, (B) IL-17A, (C) IL-10, and (D) TGF- β in each group was determined by ELISA and analyzed by the one-way ANOVA with a Tukey's post hoc test. Data are presented as the mean \pm standard error of the mean. n=5/group. *P<0.05 and **P<0.01 as indicated. C, control; M, methionine; T, treatment; WKY, Wistar-Kyoto.

establishment of the HHcy model, plasma Hcy concentration was examined in each group (Fig. 1C). Among the groups, the WKY-M group exhibited the highest plasma Hcy concentration (≤ 6 -fold higher than the other groups). Compared with the WKY-M group, the plasma Hcy concentration in the WKY-T group was significantly reduced to levels comparable with those in the WKY-C group at week 16 (Fig. 1C). In summary, these results indicated that a high methionine diet exerted a significant effect on body weight and SBP. These data also indicated that the HHcy model was successfully established.

Determination of plasma cytokine secretion and expression of related genes in brain tissue. In order to examine the effects of a high methionine diet on the main secreted factors of Th17 and Tregs in rat veins, ELISA was performed to detect the expression levels of various cytokines (IL-6, IL-17A, IL-10 and TGF- β ; Fig. 2). Compared with the WKY-C group, IL-17A secretion was increased in the WKY-M group, while the IL-10 and TGF- β levels were decreased in the WKY-M group at week 16. Following treatment, compared with the WKY-M group, IL-17A secretion in the WKY-T group was decreased, while the IL-10 and TGF- β levels were increased at week 16. In order to further verify the role of Th17 and Tregs, the levels of Tregs and Th17 cells were detected in peripheral blood at weeks 0, 4, 8, 12 and 16 using flow cytometry (Figs. 3A and 4A). Under the joint action of HHcy and hypertension, the levels of Treg were significantly inhibited, while those of Th17 cells were upregulated (Fig. 3B and 4B). Following folic acid, VitB6, and VitB12 intervention, these effects were reversed. The levels of Tregs were significantly enhanced, while those of Th17 cells were downregulated.

ROR γ t and FoxP3 are important transcription factors associated with the differentiation of Th17 and Tregs, respectively. In addition, at weeks 8, 12 and 16, fluorescent qPCR was used to detect the mRNA levels of ROR γ t, IL-17A, FoxP3 and IL-10 in the brain tissues of the three groups of rats to determine the possible regulatory changes. The results revealed that at week 16, the mRNA levels of IL-17A and ROR γ t in the WKY-M group were significantly upregulated, while the mRNA levels of FoxP3 in the WKY-M group were significantly downregulated. The mRNA levels of IL-17A and ROR γ t were downregulated in the WKY-T group. Conversely, the mRNA levels of FoxP3 in the WKY-T group increased significantly (Fig. 5). Furthermore, the protein levels of ROR γ t and FoxP3 in the brain tissues were further detected by western blot analysis (Fig. 6A and B). The relative protein expression levels of ROR γ t and FoxP3 in the WKY-M and WKY-T group were significantly higher than those in the WKY-C group. The expression of ROR γ t in the WKY-M group was higher than that in the WKY-T group. The expression of FoxP3 in the WKY-M group was significantly lower than that in the WKY-T group.

Preliminary analysis of changes associated with ischemic stroke. In order to determine whether ischemic lesions appeared in rat brain tissue, MRI imaging was performed (Fig. 7). Different from the classic thread embolization method to induce the middle cerebral artery occlusion of rats to establish a rat model of ischemic stroke, the rats were directly selected after the feeding intervention test for routine head MRI detection. The experiment did not yield a definitive positive result, indicating that no obvious damage was observed in the brain structure of each group.

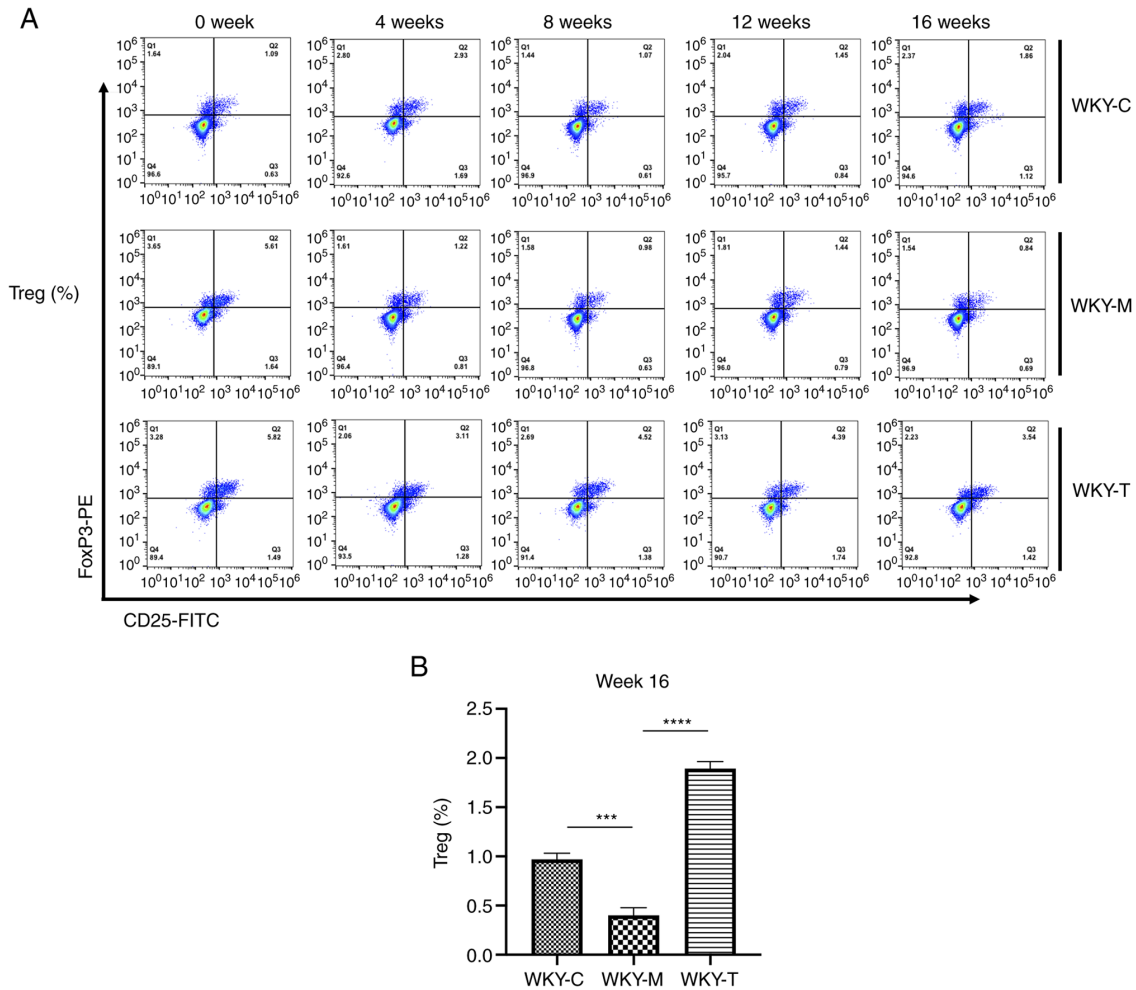


Figure 3. Flow cytometric analysis of Treg cells. CD25-FITC, FoxP3-PE and isotype control antibodies were used to determine the proportion of Treg lymphocytes. (A) Percentage of Treg cells in WKY-C, WKY-M, and WKY-T groups. (B) Percentage of Treg cells in week 16 was analyzed using the one-way ANOVA with a Tukey's post hoc test. Data are presented as the mean \pm standard error of the mean. $n=3/\text{group}$. *** $P<0.001$ and **** $P<0.0001$ as indicated. C, control; M, methionine; T, treatment; WKY, Wistar-Kyoto; Treg cells, regulatory T cells; FoxP3, forkhead box P3.

Further analysis revealed that the animal species, age and modeling method differed compared to several other classic models (36,37). Although the expected results were not obtained, the experiment did provide some experience for future use; namely that the selection of species, rat age and modeling methods need to be carefully selected.

Discussion

The blood vessels that comprise the central nervous system (CNS) vasculature have unique characteristics, termed the blood-brain barrier (BBB) (38). The precise control of CNS homeostasis by the barrier effect of the BBB allows neurons to perform appropriate functions and also protects nerve tissue from toxins and pathogens (39). At the same time, the change in barrier characteristics of the BBB has also become an important link in the pathology and development of various diseases (40-42). As regards Hcy, researchers have observed that a diet high in Hcy can lead to damage to capillaries in the hippocampal CA1 region, local and irregular thickening of the basement membrane, swelling of the mitochondria and cytoplasm, and the appearance of fibrosis in the hippocampal CA1 region (43). Another study also demonstrated that

elevated Hcy levels exerted a significant toxic effect on cerebral microvessels in the brain, indicating that Hcy was closely related to the disruption of the BBB (16). However, the specific mechanisms behind the changes caused by Hcy remain to be fully determined.

On the one hand, HHcy alters the structure and function of the BBB to increase its permeability; on the other hand, HHcy alters the function of neurons by affecting astrocytes (13,20,44). Hcy becomes the direct cause of brain tissue damage, and the inflammatory response and the permeability changes of the BBB mutually promote each other to accelerate the damage to brain tissue caused by high Hcy levels (45-49). For hypertensive patients with HHcy, current research focuses on the immune function of Th17 and Tregs (50-52). Th17 and Tregs maintain a relative balance when the body is in a normal state; however, when the body malfunctions, the balance between Th17 and Tregs is altered (21). This immune imbalance is related to the occurrence and development of a variety of diseases, such as inflammation, infection, tumors and autoimmune diseases (53).

In the present study, the systemic effects (body weight, SBP and plasma Hcy levels) of the Hcy diet were first explored. Following folic acid and vitamin B diet therapy intervention,

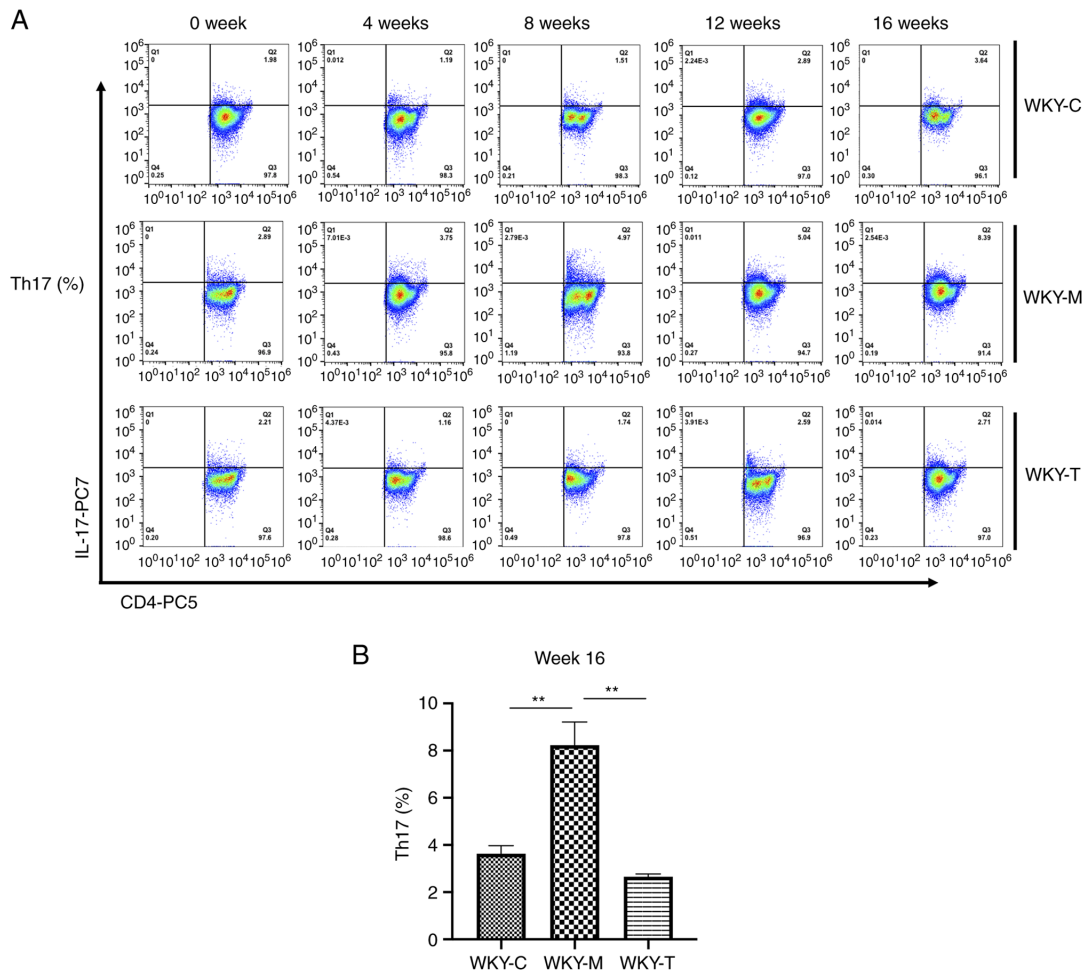


Figure 4. Flow cytometric analysis of Th17 cells. CD4-PC5, IL-17A-PC7 and isotype control antibodies were used to determine the proportion of Th17 lymphocytes. (A) Percentage of Th17 cells in WKY-C, WKY-M, and WKY-T groups. (B) Percentage of Th17 cells in week 16 was analyzed using one-way ANOVA with Tukey's post hoc test. Data are presented as the mean \pm standard error of the mean. $n=3/\text{group}$. ** $P<0.01$ as indicated. C, control; M, methionine; T, treatment; WKY, Wistar-Kyoto; Th17, T helper cell 17.

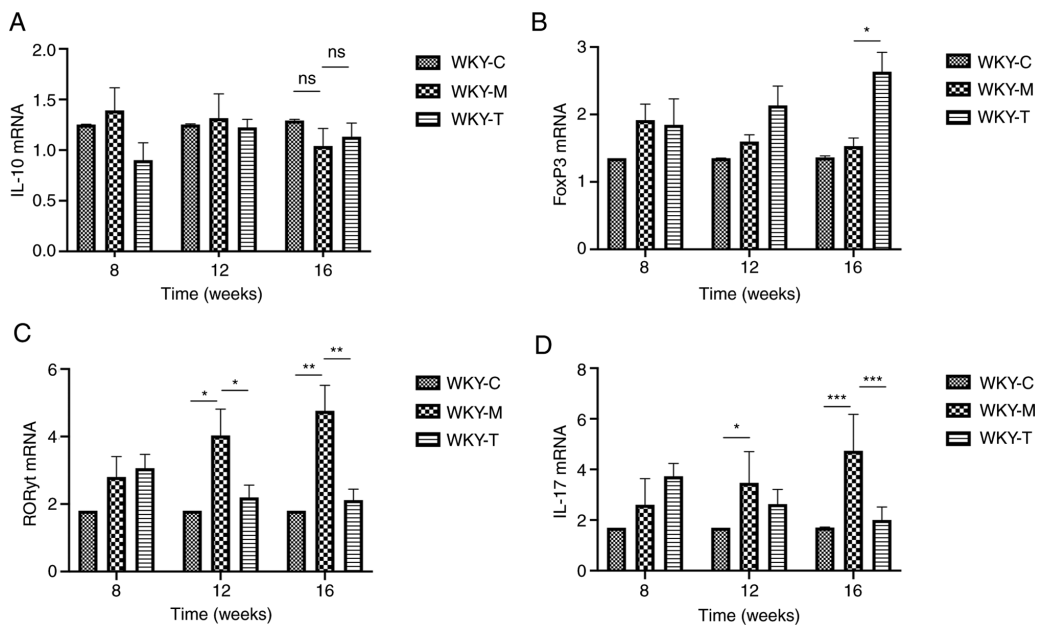


Figure 5. Expression of IL-10, FoxP3, ROR γ t and IL-17A mRNA in brain tissues. mRNA expression levels of (A) IL-10, (B) FoxP3, (C) ROR γ t and (D) IL-17A were determined by reverse transcription-quantitative PCR and normalized to β -actin gene. Data are presented as the mean \pm standard error of the mean. $n=3/\text{group}$. * $P<0.05$, ** $P<0.01$ and *** $P<0.001$ as indicated. C, control; M, methionine; T, treatment; WKY, Wistar-Kyoto; ns, no statistical significance; FoxP3, forkhead box P3; ROR γ t, retinoic acid-related orphan receptor γ t.

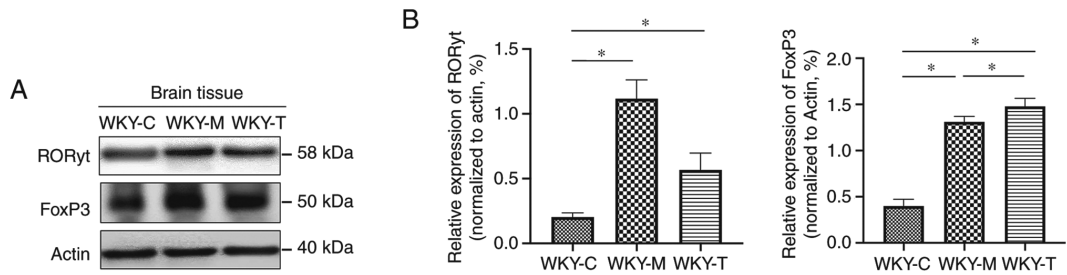


Figure 6. Protein expressions of FoxP3 and RORγt in brain tissues. (A) Western blotting results of RORγt and FoxP3 protein expression in brain tissues. (B) Relative protein expression levels of RORγt and FoxP3 were normalized to actin protein. Data are presented as the mean ± standard error of the mean. n=3/group. *P<0.05 as indicated. C, control; M, methionine; T, treatment; WKY, Wistar-Kyoto; FoxP3, forkhead box P3; RORγt, retinoic acid-related orphan receptor γ t.

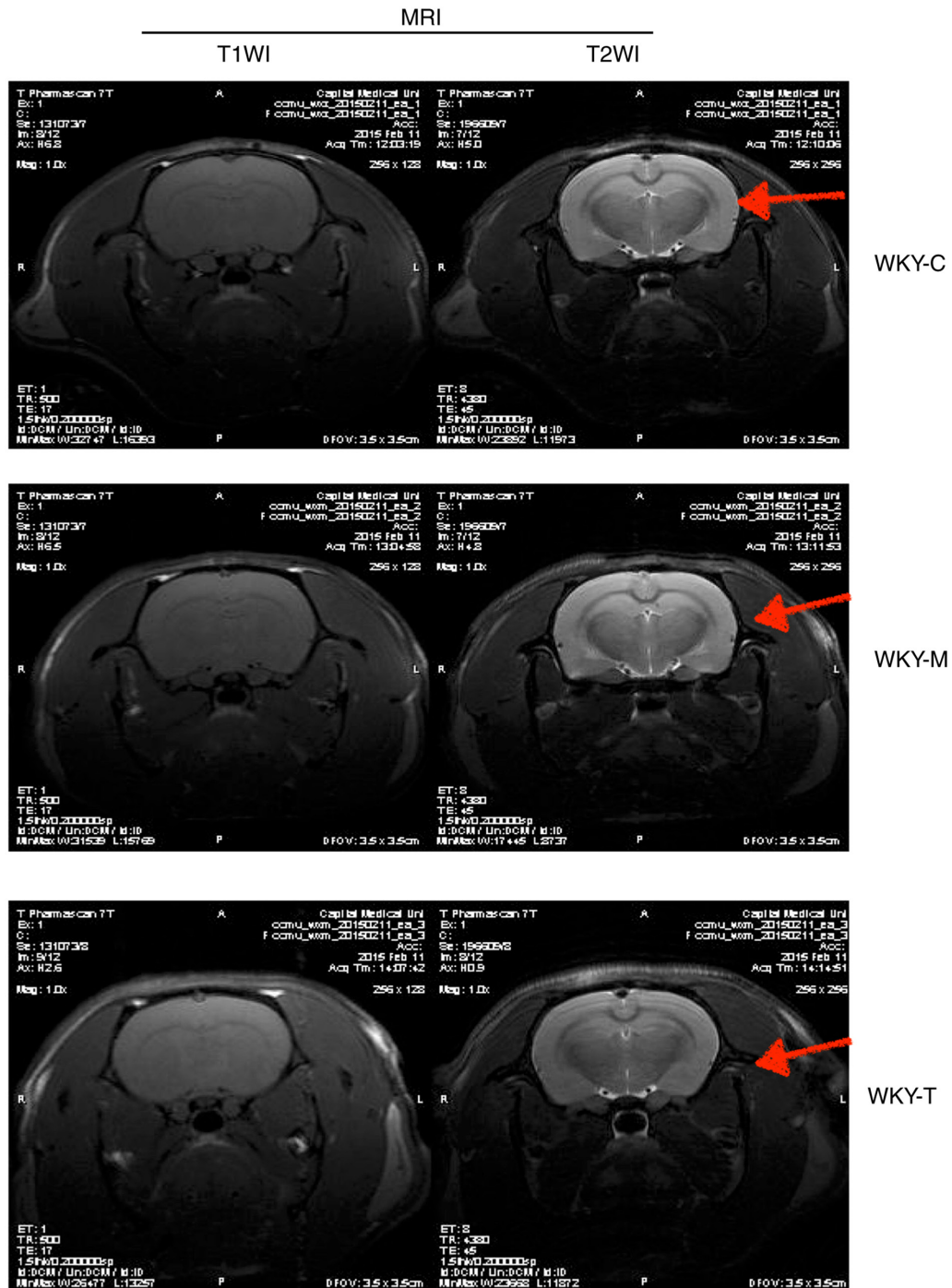


Figure 7. MRI imaging examination of brain tissues. The MRI scan was performed by T1WI sequence and T2WI sequence in each group. As indicated by the red arrows, there was no obvious damage observed in the brain structure in each group.

further analysis revealed that the expression levels of the main secretory factor, IL-17A, and the transcriptional regulator, ROR γ t, of Th17 cells in the brain tissue of the WKY-T group decreased, and returned to the corresponding levels of the normal diet group. It was demonstrated that folic acid and vitamin B treatment attenuated the effects of HHcy-induced hypertension by suppressing the role of Th17 cells and weakening the inflammatory response process. This was consistent with the findings that patients with cardiovascular disease have high blood pressure, and plasma Hcy levels are higher than in normal subjects, while folic acid, vitamin B6, vitamin B12 levels are lower than normal (54). In the present study, flow cytometry revealed that the proportion of Tregs in the WKY-M group was significantly lower than that of the normal diet group, and following folic acid and vitamin B intervention, the proportion of Tregs and the expression level of their regulatory factor, FoxP3, were increased in the WKY-T group. The results of RT-qPCR and western blot analysis revealed that the numbers of Th17 cells were decreased in the brain tissues of the WKY-T group, while those of Tregs were increased. The numbers of Th17 cells in the WKY-M group were increased gradually at 16 weeks and the protein expression of ROR γ t and FoxP3 in the brain tissues was also consistently altered. This indicated that HHcy not only enhanced the Th17 response, but also reduced the body's immune suppression mechanism by reducing the level of Tregs. Based on the current observation, dietary interventions of folic acid and vitamin B may suppress the inflammatory response process by rectifying the Th17/Treg balance, and may attenuate the adverse effects induced by hypertension. A limitation of the present study was that no differences in brain structure were observed by MRI, and the imbalance of the Treg/Th17 immune response by HHcy was detected in a preliminary perspective and not fully explained by relevant molecular mechanisms. Further studies are required to investigate the molecular mechanisms responsible for brain injury caused by HHcy. Future studies should focus on investigating the molecular mechanisms of brain injury caused by HHcy. Although any damage to the rat brain structure in the experiment was not observed, the experiment did provide certain experience for future use; namely that the selection of species, rat age and modeling methods need to be carefully selected.

In conclusion, the present study examined the effects of a high methionine diet on the main secretory factors (IL-6, IL-17A, IL-10 and TGF- β) and transcriptional regulators (ROR γ t and FoxP3) of rat Th17 and Tregs. Imaging changes of rat brain tissue and changes following folic acid and vitamin B intervention were combined, and it was found that HHcy could cause a Th17/Treg immune imbalance. This immune imbalance state was closely associated with the inflammatory response. The diet intervention (supplements of folic acid, vitamin B6 and vitamin B12) not only reduced the damage to brain tissue induced by Hcy by reducing the level of Hcy in the blood, but also reduced the inflammatory response and rectified the Treg/Th17 immune imbalance to attenuate brain tissue damage.

Acknowledgements

Not applicable.

Funding

This study was supported by Tianjin Municipal Science and Technology Commission (grant no. 16ZCZDSY03100).

Availability of data and materials

The datasets used and/or analyzed during the current study are available from the corresponding author on reasonable request.

Authors' contributions

YZ and JG carried out the experiments and drafted the manuscript. YZ, LW, XL and JG performed the statistical analysis and participated in the study design. LW and XL helped to collect data and performed the statistical analysis. YZ and JG confirm the authenticity of all the raw data. All authors read and approved the final manuscript.

Ethics approval and consent to participate

All animal experiments were approved by the Animal Experiment Ethics Committee of the Second Hospital of Tianjin Medical University (Tianjin, China), and were conducted according to the American Association for Accreditation of Laboratory Animal Care and the IACUC guidelines.

Patient consent for publication

Not applicable.

Competing interests

The authors declare that they have no competing interests.

References

- Djuric D, Jakovljevic V, Zivkovic V and Srejovic I: Homocysteine and homocysteine-related compounds: An overview of the roles in the pathology of the cardiovascular and nervous systems. *Can J Physiol Pharmacol* 96: 991-1003, 2018.
- Ganguly P and Alam SF: Role of homocysteine in the development of cardiovascular disease. *Nutr J* 14: 6, 2015.
- Spence JD: Homocysteine lowering for stroke prevention: Unravelling the complexity of the evidence. *Int J Stroke* 11: 744-747, 2016.
- McCully KS: Vascular pathology of homocysteinemia: Implications for the pathogenesis of arteriosclerosis. *Am J Pathol* 56: 111-128, 1969.
- Kim J, Kim H, Roh H and Kwon Y: Causes of hyperhomocysteinemia and its pathological significance. *Arch Pharm Res* 41: 372-383, 2018.
- Azad MAK, Huang P, Liu G, Ren W, Teklebrh T, Yan W, Zhou X and Yin Y: Hyperhomocysteinemia and cardiovascular disease in animal model. *Amino Acids* 50: 3-9, 2018.
- Capelli I, Cianciolo G, Gasperoni L, Zappulo F, Tondolo F, Cappuccilli M and La Manna G: Folic acid and vitamin B12 administration in CKD, why not? *Nutrients* 11: 383, 2019.
- Dardiotis E, Arseniou S, Sokratous M, Tsouris Z, Siokas V, Mentis AA, Michalopoulou A, Andravizou A, Dastamani M, Paterakis K, *et al*: Vitamin B12, folate, and homocysteine levels and multiple sclerosis: A meta-analysis. *Mult Scler Relat Disord* 17: 190-197, 2017.
- Pawlak R: Is vitamin B12 deficiency a risk factor for cardiovascular disease in vegetarians? *Am J Prev Med* 48: e11-e26, 2015.
- Dinavahi R and Falkner B: Relationship of homocysteine with cardiovascular disease and blood pressure. *J Clin Hypertens (Greenwich)* 6: 494-498; quiz 499-500, 2004.

11. Stehouwer CD and van Guldener C: Does homocysteine cause hypertension? *Clin Chem Lab Med* 41: 1408-1411, 2003.
12. van Guldener C, Nanayakkara PW and Stehouwer CD: Homocysteine and blood pressure. *Curr Hypertens Rep* 5: 26-31, 2003.
13. Beard RS Jr, Reynolds JJ and Bearden SE: Hyperhomocysteinemia increases permeability of the blood-brain barrier by NMDA receptor-dependent regulation of adherens and tight junctions. *Blood* 118: 2007-2014, 2011.
14. Ehrlich D and Humpel C: Chronic vascular risk factors (cholesterol, homocysteine, ethanol) impair spatial memory, decline cholinergic neurons and induce blood-brain barrier leakage in rats in vivo. *J Neurol Sci* 322: 92-95, 2012.
15. Kalani A, Kamat PK, Familtseva A, Chaturvedi P, Murdashvili N, Narayanan N, Tyagi SC and Tyagi N: Role of microRNA29b in blood-brain barrier dysfunction during hyperhomocysteinemia: An epigenetic mechanism. *J Cereb Blood Flow Metab* 34: 1212-1222, 2014.
16. Kamath AF, Chauhan AK, Kisucka J, Dole VS, Loscalzo J, Handy DE and Wagner DD: Elevated levels of homocysteine compromise blood-brain barrier integrity in mice. *Blood* 107: 591-593, 2006.
17. Le Stunff H, Véret J, Kassiss N, Denom J, Meneyrol K, Paul JL, Cruciani-Guglielmacci C, Magnan C and Janel N: Deciphering the link between hyperhomocysteinemia and ceramide metabolism in Alzheimer-type neurodegeneration. *Front Neurol* 10: 807, 2019.
18. Lee H, Kim HJ, Kim JM and Chang N: Effects of dietary folic acid supplementation on cerebrovascular endothelial dysfunction in rats with induced hyperhomocysteinemia. *Brain Res* 996: 139-147, 2004.
19. Ford TC, Downey LA, Simpson T, McPhee G, Oliver C and Stough C: The effect of a high-dose vitamin B multivitamin supplement on the relationship between brain metabolism and blood biomarkers of oxidative stress: A randomized control trial. *Nutrients* 10: 1860, 2018.
20. Kennedy DO and Haskell CF: Vitamins and cognition: What is the evidence? *Drugs* 71: 1957-1971, 2011.
21. Pirchl M, Ullrich C, Sperner-Unterwieser B and Humpel C: Homocysteine has anti-inflammatory properties in a hypercholesterolemic rat model in vivo. *Mol Cell Neurosci* 49: 456-463, 2012.
22. Zhang Y, Wang L, Zhou X, Geng J and Li X: The immunomodulatory mechanism of brain injury induced by hyperhomocysteinemia in spontaneously hypertensive rats. *J Cell Biochem* 120: 9421-9429, 2019.
23. Lee GR: The Balance of Th17 versus treg cells in autoimmunity. *Int J Mol Sci* 19: 730, 2018.
24. Crouser ED: Role of imbalance between Th17 and regulatory T-cells in sarcoidosis. *Curr Opin Pulm Med* 24: 521-526, 2018.
25. Melnik BC, John SM, Chen W and Plewig G: T helper 17 cell/regulatory T-cell imbalance in hidradenitis suppurativa/acne inversa: The link to hair follicle dissection, obesity, smoking and autoimmune comorbidities. *Br J Dermatol* 179: 260-272, 2018.
26. Hang S, Paik D, Yao L, Kim E, Trinath J, Lu J, Ha S, Nelson BN, Kelly SP, Wu L, *et al*: Bile acid metabolites control T_H17 and T_{reg} cell differentiation. *Nature* 576: 143-148, 2019.
27. Levine AG, Mendoza A, Hemmers S, Moltedo B, Niec RE, Schizas M, Hoyos BE, Putintseva EV, Chaudhry A, Dikij S, *et al*: Stability and function of regulatory T cells expressing the transcription factor T-bet. *Nature* 546: 421-425, 2017.
28. Coder B, Wang W, Wang L, Wu Z, Zhuge Q and Su DM: Friend or foe: The dichotomous impact of T cells on neuro-de/regeneration during aging. *Oncotarget* 8: 7116-7137, 2017.
29. Schmitt V, Rink L and Uciechowski P: The Th17/Treg balance is disturbed during aging. *Exp Gerontol* 48: 1379-1386, 2013.
30. Health N: Guide for the care and use of laboratory animals. NIH contract No. No1-RR-2-2135: 11-28, 1985.
31. Leary SL, Underwood W, Anthony R, *et al*: AVMA guidelines for the euthanasia of animals: 2013 edition. American Veterinary Medical Association Schaumburg, IL, 2013.
32. McGee HM, Daly ME, Azghadi S, Stewart SL, Oesterich L, Schlom J, Donahue R, Schoenfeld JD, Chen Q, Rao S, *et al*: Stereotactic ablative radiation therapy induces systemic differences in peripheral blood immunophenotype dependent on irradiated site. *Int J Radiat Oncol Biol Phys* 101: 1259-1270, 2018.
33. Livak KJ and Schmittgen TD: Analysis of relative gene expression data using real-time quantitative PCR and the 2(-Delta Delta C(T)) method. *Methods* 25: 402-408, 2001.
34. Schindelin J, Rueden CT, Hiner MC and Eliceiri KW: The ImageJ ecosystem: An open platform for biomedical image analysis. *Mol Reprod Dev* 82: 518-529, 2015.
35. Wen M, Lian Z, Huang L, Zhu S, Hu B, Han Y, Deng Y and Zeng H: Magnetic resonance spectroscopy for assessment of brain injury in the rat model of sepsis. *Exp Ther Med* 14: 4118-4124, 2017.
36. Kovalska M, Hnilicova P, Kalenska D, Tothova B, Adamkov M and Lehotsky J: Effect of methionine diet on metabolic and histopathological changes of rat hippocampus. *Int J Mol Sci* 20: 6234, 2019.
37. Jindal A, Rajagopal S, Winter L, Miller JW, Jacobsen DW, Brigman J, Allan AM, Paul S and Poddar R: Hyperhomocysteinemia leads to exacerbation of ischemic brain damage: Role of GluN2A NMDA receptors. *Neurobiol Dis* 127: 287-302, 2019.
38. Daneman R and Prat A: The blood-brain barrier. *Cold Spring Harb Perspect Biol* 7: a020412, 2015.
39. Keane J and Campbell M: The dynamic blood-brain barrier. *FEBS J* 282: 4067-4079, 2015.
40. Liebner S, Dijkhuizen RM, Reiss Y, Plate KH, Agalliu D and Constantin G: Functional morphology of the blood-brain barrier in health and disease. *Acta Neuropathol* 135: 311-336, 2018.
41. Sweeney MD, Zhao Z, Montagne A, Nelson AR and Zlokovic BV: Blood-brain barrier: From physiology to disease and back. *Physiol Rev* 99: 21-78, 2019.
42. Varatharaj A and Galea I: The blood-brain barrier in systemic inflammation. *Brain Behav Immun* 60: 1-12, 2017.
43. Lee H, Kim JM, Kim HJ, Lee I and Chang N: Folic acid supplementation can reduce the endothelial damage in rat brain microvasculature due to hyperhomocysteinemia. *J Nutr* 135: 544-548, 2005.
44. Tchanchou F, Goodfellow M, Li F, Ramsue L, Miller C, Puche A and Fiskum G: Hyperhomocysteinemia-induced oxidative stress exacerbates cortical traumatic brain injury outcomes in rats. *Cell Mol Neurobiol* 41: 487-503, 2021.
45. Faverzani JL, Hammerschmidt TG, Sitta A, Deon M, Wajner M and Vargas CR: Oxidative stress in homocystinuria due to cystathionine β -synthase deficiency: Findings in patients and in animal models. *Cell Mol Neurobiol* 37: 1477-1485, 2017.
46. Kamat PK, Kalani A, Givvimani S, Sathnur PB, Tyagi SC and Tyagi N: Hydrogen sulfide attenuates neurodegeneration and neurovascular dysfunction induced by intracerebral-administered homocysteine in mice. *Neuroscience* 252: 302-319, 2013.
47. Lehotský J, Tothová B, Kovalská M, Dobrota D, Beňová A, Kalenská D and Kaplán P: Role of Homocysteine in the ischemic stroke and development of ischemic tolerance. *Front Neurosci* 10: 538, 2016.
48. Tóthová B, Kovalská M, Kalenská D, Tomašcová A and Lehotský J: Histone hyperacetylation as a response to global brain ischemia associated with hyperhomocysteinemia in rats. *Int J Mol Sci* 19: 3147, 2018.
49. Vacek JC, Behera J, George AK, Kamat PK, Kalani A and Tyagi N: Tetrahydrocurcumin ameliorates homocysteine-mediated mitochondrial remodeling in brain endothelial cells. *J Cell Physiol* 233: 3080-3092, 2018.
50. Gao X, Li J and Chen M: Effect of homocysteine on the differentiation of CD4⁺T Cells into Th17 cells. *Dig Dis Sci* 63: 3339-3347, 2018.
51. Lin X, Meng X and Song Z: Homocysteine and psoriasis. *Biosci Rep* 39: BSR20190867, 2019.
52. Feng J, Zhang Z, Kong W, Liu B, Xu Q and Wang X: Regulatory T cells ameliorate hyperhomocysteinemia-accelerated atherosclerosis in apoE^{-/-}mice. *Cardiovasc Res* 84: 155-163, 2009.
53. Rodriguez-Iturbe B, Pons H and Johnson RJ: Role of the immune system in hypertension. *Physiol Rev* 97: 1127-1164, 2017.
54. Karolczak K, Kubalczyk P, Glowacki R, Pietruszynski R and Watala C: Aldosterone modulates blood homocysteine and cholesterol in coronary artery disease patients-a possible impact on atherothrombosis? *Physiol Res* 67: 197-207, 2018.



This work is licensed under a Creative Commons Attribution-NonCommercial-NoDerivatives 4.0 International (CC BY-NC-ND 4.0) License.